Thermal Evolution of Mercury with a Volcanic Heat Pipe Flux G. A. Peterson[1], C. L. Johnson[1,2], A. M. Jellinek[1], [1]Departmentof Earth, Ocean and Atmospheric Sciences, University of British Columbia, Vancouver, BC, V6T1Z4 (gpeterso@ubc.eosc.ca), Canada, [2]Planetary Science Institute, Tucson, AZ 85719, USA.

Introduction: Thermal evolution models for Mercury are challenged by two well-known enigmatic features unique to the innermost planet [5,14]. First, Mercury's surface is characterized by extensive structures indicative of crustal shortening. Although conventionally related to 5-10 km of radial contraction with secular cooling of the planet [2,11], cross-cutting relationships with craters suggest that ~80% of "shortening structures" formed by 3 Ga of its thermal history. Second, in addition to a present-day internally-generated magnetic field, crustal magnetic fields suggest a core dynamo was also active from 4-3.5 Ga [6]. How the present-day or past core dynamos were internally driven are still unknown [5,14].

Several papers have examined Mercury's thermal evolution using a solid-state stagnant lid models to explain the above two observations [5,14]. Here, we extend this class of thermal history calculation by considering the important additional influence of the production and advection to the surface of buoyant partial melt [9]. This picture is consistent with an extensive crustal resurfacing of Mercury to produce a crust ~20 – 50 km thick [12] by 4 Ga that forms the Intercrater Plains [4]. Inclusions of this volcanic heat flux carried by rising partial melt better explains the timing and extent of shortening structures at Mercury's surface and satisfies an additional constraint of extensive early crustal resurfacing. This mode of heat transfer has been found to be an important process on Io and Hadean Earth, and is often referred to as the Heat Pipe mechanism [9,10].

Stagnant Lid Model Set up: Mercury comprises a metallic core (radius ~2020 km) and thin (~420 km thick) mantle [14]. Initial solid-state mantle convection, driven in response to intense early radioactive heat production and partial melting, is plausibly in a stagnant lid regime [5,13,14]. Assuming quasi-steady state (SS) thermal conditions 1D parameterizations for the surface heat flux [13] enable thermal histories for the mantle and core by integrating the coupled equations [5,14]:

$$(1)\quad \rho_m C_m V_m \frac{dT_m}{dt} = -Q_m A_m + H_m V_m - Q_{vol} A_m$$

$$(2)\quad \rho_c C_c V_c \frac{dT_{cmb}}{dt} = -Q_{cmb} A_c$$

Here, T_m is the mean internal temperature of the convecting mantle, T_{cmb} is the temperature of the core-mantle boundary. ρ_m and ρ_c are the mantle and core density, C_m and C_c are mantle and core specific heat capacities. A_m, V_m and A_c are the surface area and volume of the mantle, and the surface area of the core. H_m is the heat production rate in the mantle assumed to be that of enstatite chrondrites [5,14]. Q_m is a SS surface heat flux that scales as the Rayleigh number based on the mantle layer depth D to the 1/3 power (Fig. 1). The heat flux extracted from the core Q_{cmb} depends on this heat flux and that carried down the core adiabat [5,14].

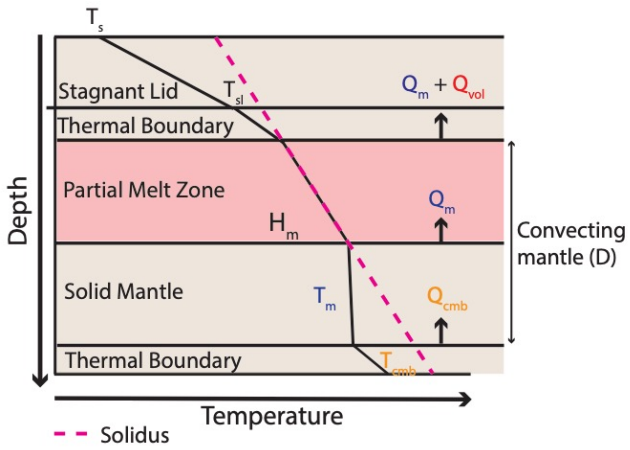

Figure 1: A diagram of the temperature profile (black solid line) used for the parameterization of mantle convection with melting included. The partial melt zone (shaded red) and heat fluxes as a function of depth used in the mantle parameterization model are shown as well.

Calculating the volcanic heat flux Q_{vol}: Q_{vol} is the advective heat flux associated with extracting partial melt out of the mantle to form crust[9,10]. Depending on the mantle melting temperature, convectively ascending mantle with temperature T_m can intersect the solidus to produce a partial melt layer (Fig. 1). For mantle rocks at or close to their solidus, melting is driven by the net power delivered to the melting region by mantle convection and retarded by the latent heat of fusion L_{fusion} [7]:

$$(3)\quad H_m M_{mz} - Q_m A_m + Q_m A_{mz} = L_{fusion} \frac{dM_{melt}}{dt}$$

M_{mz} and A_{mz} are the total mass of material and surface area at the bottom of the melt zone respectively. In Eq. (3) we assume that if T_m is greater than the solidus and if the difference between radioactive heating and power leaving the mantle by convection is positive, this excess power will go into melting to produce vertically-averaged melt fraction ø and melt volume V_{melt}.

Buoyant partial melt will rise through a combination of permeability-controlled porous media flow and

mantle convective upwelling. In the limit that porous media flow is much faster than mantle convective overturning, all partial melt rises away from the mantle and through the cold overlying lithosphere to erupt at the surface. The temperature profile within the partial melt zone is that of the solidus and we establish an upper bound for this contribution to the surface heat flow (Fig 1).

Model without Q_{vol}: Fig. 2 shows the thermal evolutions of the mantle and core and the associated radial thermal contraction ΔR (calculated as in [14]). The results are similar to those in [5] and [14] and cannot explain the following observations:

1) Why ~80% of shortening structures formed by 3 Ga [1,3]. This model predicts that contraction (and by inference the associated shortening structures) occurred continuously over Mercury's evolution.

2) The presence of a global magnetic field today or at ~3.9 Ga [6], if the dynamo is driven by thermal convection alone. To have a magnetic field, Q_{cmb} must be at least as large as the core's adiabatic heat flux, which is likely ~15 – 20 mWm^2 [5]. Fig. 2b shows that Q_{cmb} quickly falls below this range by 4.25 Ga.

Model with Q_{vol} :The inclusion of Q_{vol} into a stagnant lid thermal evolution makes progress. First, the mantle interior temperature T_m decreases to below the solidus by 3.5 Ga, resulting in a ΔR of ~6 km (Fig. 1c). This occurs because Q_{vol} is largest when H_m is maximum early in the evolution, which allows ø and q to reach maxima of 6% and 0.5 mm/yr, respectively. These predictions are consistent with most shortening structures forming early in Mercury's evolution [1,3], as well as the crustal resurfacing responsible for the Intercrater plains.

Second, the model allows a magnetic field to continue to until 3.5 Ga, consistent with crustal magnetic field studies (with or without inner core solidification). This model does not predict conditions that favor a present day thermally-driven dynamo field.

Future Work:

1) Due to Mercury's thin mantle a switch from convection to conduction within the planet's thermal evolution is an expected consequence of cooling and melt extraction. The implications for the distribution and timing of shortening structures as well as magnetic field generation are unknown.

2) This model does not include inner core growth, which would extend the longevity of the thermal dynamo predicted in Figure 2.

3) An inherent limitation of a 1D thermal evolution models is that melt will erupt uniformly across the lithosphere. The extent to which this simple picture is justified through, say, a symmetric or homogeneous distribution of shortening and volcanic features across Mercury's surface is unknown.

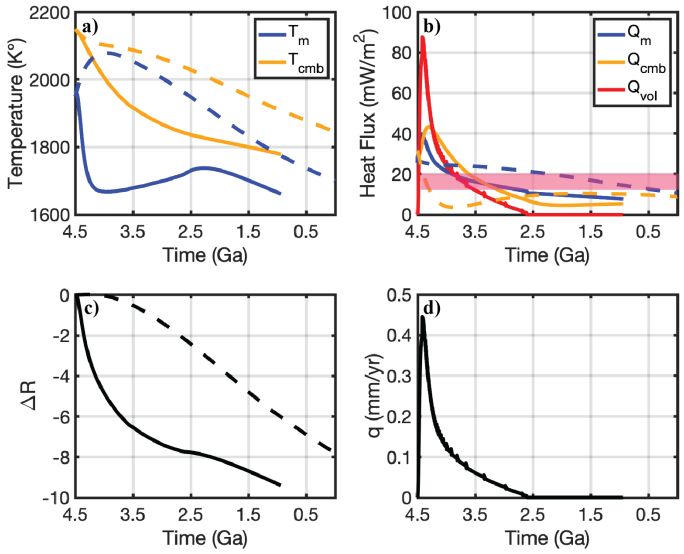

Figure 2: a) and b) show the evolution of T_m and Q_m in blue and T_{cmb} and Q_{cmb} in yellow. Q_{vol} is in red in b). The shaded pink region in B) is the minimum Q_{cmb} heat flux that allows a dynamo to stay on. The radius change as a function of time is shown in c). In panels A - C the stagnant lid model with Q_{vol} set to zero is the dashed line and the solid line is when Q_{vol} is added. d) is the discharge rate (q) of the partial melt zone with time.

References: [1] Banks (2015) J. Geophys. Res. Planets, 120, 1751–1762 [2] Byrne et al. (2014) *Nature Geosci*., 7, 301-307 [3] Crane and Klimczak (2017)., Geophys. Res. Lett., 44, [4] Deveni (2018)., *Cambridge Univ. Press* [5] Hauck (2018)., *Cambridge Univ. Press* [6] Johnson et al., (2015) Science, 348, 892–895. [7] Mckenzie (1984)., *Cambridge Univ. Press* [8]Miller et al., (2014) *Elsevier 388 273-282* [9]Moore and Webb (2013) *Nature* 501, 501–505 [10] O'Reilly and Davies (1981*) Geophys. Res. Lett,* 8, 313 – 316. [11] Peterson et al., (2019) Geophys. Res. Lett., 44 [12] Phillips (2018)., *Cambridge Univ. Press* [13] Solomatov and Moresi (2000) *J. of Geophys Res.,* 105, 21,795-21,817 [14] Tosi et al. (2015) *Geophys. Res. Lett*., 42, 7327-7335.